Research article

Knockdown of TTC9 inhibits the proliferation, migration and invasion, but induces the apoptosis of lung adenocarcinoma cells

Xiaoyue Huang [a,d,1], Lingyu Jiang [b,c,1], Zhaoke Wen [d], Mingqing Yuan [a,**], Yonglong Zhong [d,*]

[a] Medical College, Guangxi University, Nanning 530021, PR China
[b] The First Affiliated Hospital, Jinan University, Guangzhou 510006, PR China
[c] Intensive Care Unit, The People's Hospital of Guangxi Zhuang Autonomous Region, Guangxi Academy of Medical Sciences, Nanning 530021, PR China
[d] Department of Thoracic Surgery, The People's Hospital of Guangxi Zhuang Autonomous Region, Guangxi Academy of Medical Sciences, Nanning 530021, PR China

ARTICLE INFO

ABSTRACT

Lung adenocarcinoma (LUAD) is one of the most commonly diagnosed subtypes of lung cancer, and one of the deadliest cancers. Tetratricopeptide repeat domain 9A (TTC9) is upregulated and has played an oncogenic role in some malignant tumors. However, the expression and role of TTC9 has not yet been elucidated in LUAD. Here, we investigated the expression profiles, biological functions and potential molecular mechanism of the TTC9 gene in LUAD. TTC9 expression was significantly overexpressed in LUAD tissues compared with that in normal lung tissues. TTC9 expression was closely correlated with gender, lymph node metastasis, and survival status in the TCGA-LUAD cohort. Subsequent cellular function assays demonstrated that knockdown of TTC9 promoted PC9 cell apoptosis and inhibited cell proliferation, migration and invasion, leading to cell cycle arrest in G2 phase. Moreover, inhibition of TTC9 suppressed the tumorigenicity of PC9 cells in nude mice. TTC9 might serve as oncogene in LUAD through cancer-related signaling pathways including p38 MAPK pathway. The expression of TTC9 gene might be modulated by DNA copy number variant and DNA methylation. TTC9 was significantly associated with tumor immune infiltration patterns. Accordingly, TTC9 may be a novel therapeutic target for the treatment of LUAD.

1. Introduction

As of 2020, lung cancer was the leading cause of cancer-related death globally [1]. More than 85% of lung cancer patients are diagnosed with non-small-cell lung carcinoma, with lung adenocarcinoma (LUAD) being the most commonly identified histological type. LUAD-associated morbidity and mortality have increased yearly over the past decade, which may be associated with environmental pollution, occupational hazards, lifestyle, and carcinogenic factors associated with atypical adenomatous hyperplasia of the lung [2, 3, 4]. Despite the recent progress in the diagnosis and treatment of LUAD, the long-term outcome of patients remains poor. The 5-year overall survival (OS) rate is below 20% [3]. Combined, these observations emphasize the need to further explore therapeutic targets of LUAD so as to improve the prognosis and treatment of LUAD patients.

From previous research, Cao et al [5] found the human tetratricopeptide repeat domain 9 (TTC9) gene is located on chromosome 14q24.2 and encodes a transcript that is 5094 bp long. They found that TTC9 was aberrantly expressed in variate of human tissues, including the colon, heart, kidney, lung, and pancreas. TTC9 in MCF-7 cells were also regulated by p38 kinase inhibitor SB203580 and hormones. Researchers also found that Tropomyosin Tm5NM-1 was identified as one of the TTC9 paired proteins [6, 7]. Tm5NM1, a member of the cytoskeletal tropomyosin family, binds the actin-binding protein Fascin and regulates actin filament polymerization/depolymerization, which contributes to changes in focal adhesion and is thought to be related to the regulation of mesenchymal cells movement [8, 9]. Therefore, TTC9 may be plays a critical role in cancer cell invasion and distant metastasis [10].

However, the expression profile and biological role of TTC9 in LUAD are rarely reported. Hence, we investigated the expression profile and

role of TTC9 in LUAD using bioinformatics, clinical paraffin specimens, a series of *in vitro* cell experiments, and the nude mouse subcutaneous tumorigenesis model.

2. Materials and methods

2.1. Tissue sample

Tumor tissues and paired normal lung tissues (>5 cm away from tumors) were obtained from patients undergoing LUAD surgery in 2015–2017 at the People's Hospital of Guangxi Zhuang Autonomous Region (Nanning, China). All participants did not receive radiotherapy, chemotherapy, or immunotherapy pre-operatively. The above mentioned LUAD tissues and non-tumor tissues were confirmed by experienced pathologists. The histopathological results were reviewed by two independent experienced pathologists.

2.2. Immunohistochemistry

After grilling, tissue slices were dewaxed with xylene and rehydrated via a graded ethanol series. For antigen retrieval, the slices were boiled with $1\times$ citric acid solution (pH 6.0, Solarbio Science & Technology, Beijing, China) in a pressure cooker for 3 min and then were cooled to room temperature (RT). To block endogenous peroxidase activity, the slices were incubated with 3% H_2O_2 for 20 min. Subsequently, the slices were blocked with goat serum for 15–20 min, and then incubated with rabbit anti-human TTC9 polyclonal antibody (1:100; code: SAB1301612; Sigma-Aldrich, Burlington, Massachusetts, USA) at 4 °C overnight. For displaying antigen distribution, the slices were incubated with the ready Max Vision reagent (Fujian Maixin Biotechnologies, Fuzhou, China) under RT conditions. The freshly prepared 3,3′- diaminobenzidine solution was slowly dripped into the slices for color reaction, and then hematoxylin staining was performed. The slices were subsequently differentiated in hydrochloric acid and immersed in an ammonia solution. After dehydrating and sealing, the slices were observed and photographed under a light microscope (Olympus, Tokyo, Japan).

2.3. Mining The Cancer Genome Atlas database transcriptome sequencing data

The RNA-seq data from The Cancer Genome Atlas (TCGA; https://cancergenome.nih.gov/) [11] database was integrated to analyze the expression profile of TTC9 mRNA. A total of 514 cases of primary LUAD and 59 normal lung controls were extracted for bioinformatics analysis. Among 514 LUAD patients, 505 cases of patients had complete clinicopathological characteristics and follow-up information. The clinical information included age, gender, smoking history, tumor size (T), lymph node invasion (N), distant metastasis (M), clinical stage (TNM), recurrence status, residual tumor, and outcome. The follow-up information included overall survival (OS), progression-free interval (PFI), disease-free interval (DFI), and disease-specific survival (DSS).

2.4. Genetic and epigenetic analysis of TTC9 in LUAD

To explore the possible mechanism underlying the role of TTC9 in LUAD, data on copy number variation (CNV) and DNA methylation levels (methylation 450k) were simultaneously obtained from TCGA. Data on TTC9 mRNA expression, CNV, and DNA methylation levels in LUAD cell lines were collected from the Cancer Cell Line Encyclopedia (CCLE) (https-dashela.broad institute.org/ccle) [12, 13], an online public database for genomic data visualization and analysis for more than 1,100 cell lines. UALCAN database (http://ualcan.path.uab.edu) [14] was used to analyze the level of TTC9 promoter methylation in LUAD.

2.5. Analysis of differentially expressed genes correlation with TTC9

We used LinkedOmics (http://www.linkedomics.org) [15], a public bioinformatics portal that provides multi-omics data across all 32 TCGA cancer types, to identify the differentially expressed genes (DEGs) associated with TTC9 in TCGA-LUAD cohort. A Benjamini and Hochberg false discovery rate (FDR) < 0.01 and P < 0.05 were set as the threshold criteria. Correlation analysis was performed using GEPIA2 (http://gepia2.cancer-pku.cn) [16], a public online interactive platform that can be used to process RNA-seq data of various human solid tumor and normal samples from TCGA and GTEx databases. The test method was Spearman's rank correlation test in the analysis. LUAD patients were divided into high and low expression groups by the median values of TTC9 mRNA expression.

2.6. Tumor microenvironment analysis

Several algorithms including xCELL (http://xcell.ucsf.edu/) [17], EPIC (https://gfellerlab.shinyapps.io/EPIC_1-1/) [18], CIBERSORT (https://cibersort.stanford.edu/) [19], quanTiseq (https://icbi.i-med.ac.at/software/quantiseq/doc/index.html) [20], MCP-counter (https://github.com/ebecht/MCPcounter) [21, 22], TIDE [23], TIMER (https://cistrome.shinyapps.io/timer/) [24] were used to evaluate the correlation between TTC9 expression and tumor-infiltrating immune cells in LUAD. TIMER is a common web tool for evaluating immune infiltration of different cancer types. The relationship between tumor immune infiltration of LUAD and patients' survival was analyzed using the TIMER database.

TISIDB, a comprehensive portal for tumor-immune interactions, was used to analyze the expression of TTC9 gene in different immune subtypes. The immune subtypes included C1 (wound healing), C2 (interferon-gamma dominant), C3 (inflammation), C4 (lymphocyte depletion), C5 (immune silent) and C6.

2.7. Gene set enrichment analysis

The LinkInterpreter module of LinkedOmics [25] was used to perform gene set enrichment analysis (GSEA). RNA-seq data extracted from TCGA was used for GSEA analysis in terms of the Gene Ontology (GO) and the Kyoto Encyclopedia of Genes and Genomes (KEGG). GO included cellular components, molecular functions, and biological processes. The thresholds were set as follows: FDR <0.05 and P < 0.05.

2.8. Cell source and culture

The human LUAD cell lines including PC9, A549, H1299, and NCI-H1975 were purchased from the Typical Culture Preservation Committee of the Chinese Academy of Sciences (Shanghai, China). The human normal lung epithelial cells BEAS-2B was obtained from Shanghai Zhongqiao Xinzhou Biotechnology Co., Ltd. All cells were cultured in RPMI 1640 medium containing 10% fetal bovine serum and 1% streptomycin at 37 °C with 5% CO_2. The above reagents were purchased from Thermo Fisher Scientific Inc. (Waltham, MA, USA).

2.9. Lentivirus design and transfection

The GV248-GFP-shRNA-TTC9 lentiviral vector was obtained from Shanghai GeneChem Co., Ltd (Shanghai, China). The target sequences of short hairpin RNAs (shRNA) for knockdown TTC9 (sh-TTC9) was 5′-CGTGAAGCCATAGGCAAAT-3′. A GV248-GFP-lentiviral vector (5′-TTCTCCGAACGTGTCACGT-3′) was used as a negative control (sh-NC). Cell transfection of shRNA was performed according to the manufacturer's instructions.

2.10. RNA extraction and mRNA detection

Total RNA was extracted using Trizol reagent (Solarbio biotechnology, Beijing, China) following the manufacturer's protocol. The extracted RNA was reverse transcribed into cDNA using a reverse transcription kit (Takara Bio Inc, Tokyo, Japan). Real-time quantitative polymerase chain reaction (qPCR) was performed in an ABI 7500 real-time quantitative fluorescent PCR system (Applied BioSystems, Carlsbad, USA). The sequences of the primers (purchased from Sangon Biotech, Shanghai, China) used for qPCR were as follows: For TTC9, 5′-GTCTCATGGGCTGGGATGCT-3′ forward and 5′-CTGCTGCCTGTGGGA TGGTA-3′ reverse; and for GAPDH 5′-CATGAGAAGTATGACAACAGCCT-3′ forward and 5′-AGTCCTTCCACGATACCAAG-3′ reverse. The RT-qPCR assay was repeated three times. Relative gene expression levels were calculated using the $2^{-\Delta\Delta CT}$ method.

2.11. Cell Counting Kit-8 assay

Cells were cultured in 96-well culture plates and examined at 0, 24, 48, 72, and 96 h by Cell Counting Kit-8 reagent (CCK-8, Dojindo, kumamoto, Japan). CCK-8 reagent (20 μl) was added to each well (1,500 cells per well), followed by incubation for 2 h in the dark. Finally, the optical density of each well was determined at 450 nm using a microplate reader (Thermo Scientific, Waltham, MA, USA).

2.12. Wound healing assay

Approximately 5×10^5 cells were seeded in each well of a six-well plate to >90% confluence. Horizontal lines were evenly marked (every 0.5–1 cm) on the back of the plate. Scratches were made across the cell layer. At 0, 12, and 24 h, images were captured under a microscope. The cell migrative rate was analyzed using ImageJ software (National Institutes of Health, Bethesda, MD, USA).

2.13. Transwell migration assay

Collected cells and adjusted their density to 1×10^5. Cell migratory ability was assessed in a 24-well culture plate using Transwell inserts (Corning Inc., Corning, NY, USA). RPMI 1640 medium containing 15% serum (600 μl) was added to the lower chamber of each insert while a cell suspension (200 μl) in 5% fetal bovine serum medium was added to the upper chamber. Cells were incubated at 37 °C with 5% CO_2 for 18–24 h. After removing the fluid and un-migrated cells, cells in the lower chamber (migrated cells) were fixed in methanol and then stained with of 0.1% crystalline violet. The lower membrane of the chamber was carefully obtained and was transferred to a glass slide. The number of cells invading the membrane was counted in five randomly selected visual fields under a microscope (Olympus, Tokyo, Japan).

2.14. Cell invasion assay

BioCoat Matrigel invasion chambers (24-well plate, Corning Inc.) were used for the cell invasion assay. Cells were collected and cell density was adjusted to 1×10^5 cells/ml. The upper compartment of the chambers was filled with serum-free medium (200 μl) for rehydration for 30 min. Subsequently, 200 μl of a cell suspension (adjusted to 1×10^5 cells/ml) in serum-free medium was added to the upper chamber while complete medium containing 15% serum (600 μl) was added to the lower chamber. The cells were incubated at 37 °C with 5% CO_2 for 30–34 h. The following steps were similar to the migration assay.

2.15. Apoptosis and cell cycle assay

Annexin V-allophycocyanin (AV-APC)/propidium iodide (PI) (KeyGen Biotech, Nanjing, China) staining was performed to detect cell apoptosis by flow cytometry. After centrifugation, PC9 cells ($3–5 \times 10^5$/ml) were re-suspended in binding buffer (500 μl), incubated with Annexin V-allophycocyanin (5 μl) for 5–10 min, and then mixed with PI dye solution (5 μl) in the dark for 5–15 min at RT. After incubation, flow cytometry (BD Biosciences, Franklin Lakes, USA) was performed, and FlowJo v10 software was used to analyze the data. Similarly, LUAD cells were fixed in 75% ethanol and disposed overnight at −20 °C. The following day, the cells were stained with Cell Cycle Staining Kit (Multi Sciences Biotech Co., Ltd, Hangzhou, China) (0.5 ml) in the dark for 30 min at RT, thoroughly mixed, and detected by flow cytometry within 1 h. The results were analyzed using ModFit LT v.3.1 software.

2.16. Western blot

Total protein was extracted from cells using protein lysate assay buffer (Biyuntian, Beijing, China) supplemented with 10 g/L PMSF (protease inhibitor; Biyuntian) and 10 g/L phosphatase inhibitor (Yeasen Biotechnology, Shanghai, China). A BCA protein assay kit (Biyuntian) was used to examine protein concentration. Equal amounts of protein were separated by 12.5% sodium dodecyl sulfate-polyacrylamide gel electrophoresis (SDS-PAGE). The separated protein was transferred to a polyvinylidene difluoride membrane (PVDF). After blocking with Tris-buffered saline with Tween 20 (TBST) containing 5% nonfat milk for 2 h at RT, the membrane was incubated with primary antibodies against TTC9 (1:500; SAB1301612; Sigma-Aldrich, St. Louis, MO, USA); phosphorylated -p38 (1:1,000, 4511S, Cell Signaling Technology (CST), Danvers, MA, USA), caspase-3 (1:1000, 9662S, CST), p38 MAPK (1:4000, 66234-1-lg, Proteintech, Chicago, IL, USA), BAX (1:5000, 50599-2-lg, Proteintech), β-tubulin (1:5000, 10094-1-AP, Proteintech), E-cadherin (1:5000, 20874-1-AP, Proteintech) and N-cadherin (1:2000, 22018-1-AP, Proteintech). Following incubating with primary antibody, these membranes were diluted overnight in TBST at 4 °C. After washing with TBST, these membranes were incubated with horseradish peroxidase-labeled anti-rabbit antibodies (1: 2,000, GB233303-1; Bioss, Beijing, China) for 2 h at RT. Protein bands were visualized using the enhanced chemiluminescence Western blot detection reagent (Biosharp, Hefei, China) on the Odyssey FC imaging system (LI-COR, Biosciences, USA). The density of the bands was analyzed and quantified using ImageJ software.

2.17. Animal experiment

The BALB/C female nude mice were purchased from the Laboratory Animal Center, Guangxi Medical University. Twelve female mice (five weeks old), raised under specific-pathogen-free conditions, were randomly divided into two groups (sh-NC vs. sh-TTC9, n = 6/group) according to body weight. A total of 2×10^6 transfected cells were subcutaneously injected into the right armpit of each mouse. Twenty-one days after inoculation, mice were euthanized by cervical dislocation. The final weight was measured and tumor volume was calculated using following formula: (length $\times$ width^2)/2.

2.18. Statistical analysis

In the present study, SPSS 20.0 software (IBM Corporation, Armonk, NY, USA) was used for statistical analysis. Wilcoxon rank sum test and Welch's t-test was conducted to compare the differences between groups. Pearson correlation and Spearman's rank correlation were used to examine the correlation. TCGA-LUAD dataset was divided into a low

TTC9 expression group and a high TTC9 expression group according to the gene expression of TTC9. The median values of TTC9 mRNA were instead of duplicated data. GraphPad Prism 8.0.2 (GraphPad Software Inc., San Diego, CA, USA) was conducted for the Log-rank test, Cox regression analysis and Kaplan-Meier curves. $P < 0.05$ was considered statistically significant.

2.19. Ethics statement

The present study was approved by the Ethics Committee/Institutional Review Committee of the People's Hospital of Guangxi Zhuang Autonomous Region (Number: KY-GZR-2019-043). All participants provided written informed consent according to the Declaration of Helsinki. Animal experiment was approved by the Animal Care Committee of Guangxi Medical University (approval number: 202103022) and carried out according to the National Research Council's Guide for the Care and Use of Laboratory Animals (NIH Publications No. 8023, revised 1978).

3. Results

3.1. TTC9 was highly expressed in LUAD

We extracted the RNA-seq data for TTC9 from TCGA pan-cancer dataset and analyzed TTC9 mRNA expression levels in primary tumors and corresponding normal solid tissues (sample size ≥3). As shown in Figure 1A, TTC9 mRNA expression levels were significantly higher in most solid malignant tumors including LUAD than that in corresponding normal tissues ($p < 0.001$). These observations suggested that TTC9 expression is overexpressed in most malignant solid tumors. TTC9 might be involved in the process of tumor occurrence and progression. We also analyzed the expression levels of TTC9 protein in paraffin-embedded LUAD tissue using immunohistochemistry. TTC9 protein was mainly expressed in the cytoplasm of cancer cells. TTC9 protein staining was strong in tumor tissue but weak in alveolar epithelial cells of normal lung tissue (Figure 1B–E). These results indicated that TTC9 was overexpressed in patients with LUAD.

3.2. TTC9 expression was associated with malignant clinicopathologic features of LUAD

According to the median value of TTC9 mRNA expression, the TCGA-LUAD cohort was divided into high TTC9 expression group and low TTC9 expression group, and the relationship between TTC9 mRNA expression and the clinical features was analyzed. As shown in Table 1, TTC9 mRNA expression levels were significantly higher in female patients ($p = 0.045$), cases with positive lymph node metastasis ($p = 0.018$), and dead cases ($p = 0.014$). But, high TTC9 mRNA expression was not related to age, smoking history, tumor size, distal metastasis, TNM stage, or

Figure 1. TTC9 was overexpressed in LUAD. (A) Pan-cancer expression of the TTC9 gene based on data from TCGA data. (B–E) Immunohistochemical staining of TTC9 in normal lung tissue and tumor tissue. Representative IHC staining images of TTC9 protein in (B) normal lung tissue and (C–E) LUAD tissues (×200 magnification, Scale bars: 50 μm). (B) Negative staining in normal lung tissue; (C) weak staining, (D) medium staining, and (E) strong staining in LUAD tissue, respectively. The correlation between the TTC9 mRNA expression level and clinicopathologic characteristics relating to LUAD patient data available in TCGA-LUAD cohort. (F) Tumor tissues and normal tissues, (G) sex, (H) tumor size, (I) lymph node metastasis, (J) distant metastasis, (K) TNM stage, (L) survival status, and (M) residual tumor. Kaplan-Meier curves for (N) OS, (O) DFI, (P) DSS, and (Q) PFI. Welch's t test and Wilcoxon rank sum test were used. *$p < 0.05$, **$p < 0.01$, ***$p < 0.001$.

Table 1. The association of the clinicopathological parameters between high and low TTC9 mRNA expression groups in TCGA-LUAD patients.

Parameters	Variables	TTC9 mRNA expression		χ^2/t	p-value
		Low (n = 252)	High (n = 253)		
Age (years)	>65	131	126	0.162	0.687
	≤65	117	121		
	Null	4	6		
Gender	Male	128	106	4.018	0.045*
	Female	124	147		
Smoking History	1	32	40	1.004	0.316
	2/3/4/5	213	206		
	Null	7	7		
T classification	T1–2	221	217	0.287	0.592
	T3–4	30	34		
	Tx/null	1	2		
Nodal invasion	N0	174	151	5.633	0.018*
	N1/2/3	71	97		
	Nx/null	7	5		
Distant metastasis	M0	173	164	1.496	0.221
	M1	16	9		
	Null	63	80		
Clinical stage	I/II	197	193	0.748	0.387
	III/IV	49	58		
	Discrepancy/null	6	2		
Residual tumors	R0	164	172	3.470	0.062
	R1/R2	4	12		
	Rx/null	84	69		
Living status	Living	174	148	6.081	0.014*
	Dead	78	105		

Smoking history: 1: lifelong non-smoker; 2: current smoker; 3. current reformed smoker (for >15 years); 4. current reformed smoker (for ≤15 years); 5. Current reformed smoker (duration not specified); R0: no residual tumor; R1: microscopic residual tumor; R2: macroscopic residual tumor; RX: the presence of residual tumor cannot be assessed; null: no data. *: p < 0.05. TCGA: The Cancer Genome Atlas. LUAD: lung adenocarcinoma.

residual tumor. These results indicated that the TTC9 mRNA expression level was significantly correlated with sex, lymph node metastasis, and survival status. Then, we extracted RNA-seq data and used scatterplots to show the relationship between TTC9 mRNA expression and clinicopathologic parameters. As shown in Figure 1F, the expression level of TTC9 mRNA was significantly higher in LUAD tissue than that in normal tissue (p < 0.001). Moreover, TTC9 mRNA expression was obviously upregulated in females, cases with positive lymph node metastasis, dead cases, and cases with residual tumor (Figure 1G, I, L, M, p < 0.05). Otherwise, TTC9 mRNA expression was not associated with tumor size, distant metastasis, or TNM staging (Figure 1H, J, K).

3.3. High TTC9 expression was associated with poor prognosis in patients with LUAD

We further explored the relationship between TTC9 expression and patients' outcome including OS, PFI, DFI, and DSS in the TCGA-LUAD cohort. Kaplan-Meier curves showed that LUAD patients who had high TTC9 expression levels had significantly poorer OS, DFI, DSS, and PFI (p = 0.0166, p = 0.0010, p = 0.0299, and p = 0.0001, respectively) (Figure 1N–Q). Subsequently, a Cox regression analysis was performed to assess the prognostic value of TTC9 in LUAD. Univariate regression analysis revealed that patients' OS was significantly correlated with TTC9 mRNA expression (p = 0.014), clinical stage (p < 0.001), and residual tumor (p < 0.001). Multivariate regression analysis demonstrated that TTC9 mRNA expression (p = 0.032) as well as clinical stage (p < 0.001), and residual tumor (p < 0.001) were independent prognostic factors for reduced OS in LUAD (Table 2).

Moreover, univariate analysis demonstrated that residual tumor (p = 0.017) and TTC9 mRNA expression (p = 0.001), but not sex, age, or smoking history (all p > 0.05), were associated with DFI. Multivariate analysis further indicated that residual tumor (p = 0.008) and TTC9 mRNA expression (p = 0.001) were independent risk factors for a shorter DFI in LUAD (Table 3). In terms of DSS, univariate analysis revealed that clinical stage, residual tumor, and TTC9 mRNA (p < 0.001, p < 0.001, and p = 0.031, respectively) were correlated with DSS. Multivariate regression analysis confirmed that clinical stage and residual tumor (p < 0.001 and p = 0.001, respectively) were independent risk factors for poorer DSS in LUAD (Table 4). Univariate regression analysis revealed that clinical stage (p < 0.001), as well as residual tumor (p < 0.001) and TTC9 mRNA expression (p = 0.003), but not sex, age, or smoking history (all p > 0.05), were correlated with PFI. Furthermore, multivariate regression analysis suggested that clinical stage (p = 0.038), residual tumor (p = 0.002), and TTC9 mRNA expression (, p < 0.001) were independent risk factors for a shorter PFI in LUAD (Table 5). Collectively, these findings indicated that high TTC9 mRNA expression was negatively correlated with OS, DFI, and PFI in patients with LUAD.

Table 2. Univariate and multivariate analysis of OS in TCGA-LUAD patients.

	Univariate analysis				Multivariate analysis			
Parameters	HR	95% CI (lower/upper)		P	HR	95% CI (lower/upper)		P
Age (continuous)	1.008	0.992	1.023	0.330				
Gender								
Female vs. Male	0.938	0.702	1.255	0.669				
Smoking history								
Smoker vs. non-smoker	0.912	0.604	1.377	0.661				
Clinical stag								
III/IV vs. I/II	2.651	1.945	3.613	<0.001*	2.471	1.800	3.392	<0.001*
Residual tumors								
Yes vs. No	3.937	2.204	7.033	<0.001*	2.782	1.536	5.037	0.001*
TTC9 expression								
High vs. low	1.443	1.076	1.935	0.014*	1.384	1.029	1.861	0.032*

Smoking history: 1: lifelong non-smoker; 2: current smoker; 3. current reformed smoker (for >15 years); 4. current reformed smoker (for ≤15 years); 5. Current reformed smoker (duration not specified); HR: Hazard ratio. *: p < 0.005.

Table 3. Univariate and multivariate analysis of DFI in TCGA-LUAD patients.

Parameters	Univariate analysis				Multivariate analysis			
	HR	95% CI (lower/upper)		P	HR	95% CI (lower/upper)		P
Age (continuous)	1.016	0.994	1.039	0.158				
Gender								
Female vs. Male	0.814	0.536	1.237	0.335				
Smoking history								
Smoker vs. non-smoker	0.742	0.436	1.263	0.272				
Clinical stage								
III/IV vs. I/II	0.803	0.371	1.740	0.578				
Residual tumors								
Yes vs. No	4.108	1.281	13.170	0.017*	4.913	1.523	15.850	0.008*
TTC9 expression								
High vs. low	2.033	1.321	3.128	0.001*	2.044	1.323	3.158	0.001*

Smoking history: 1: lifelong non-smoker; 2: current smoker; 3: current reformed smoker (for >15 years); 4: current reformed smoker (for ≤15 years); 5: current reformed smoker (duration not specified); HR: Hazard ratio. *: $p < 0.005$.

Table 4. Univariate and multivariate analysis of DSS in TCGA-LUAD patients.

Parameters	Univariate analysis				Multivariate analysis			
	HR	95% CI (lower/upper)		P	HR	95% CI (lower/upper)		P
Age (continuous)	0.988	0.970	1.007	0.206				
Gender								
Female vs. Male	1.040	0.716	1.512	0.836				
Smoking history								
Smoker vs. non-smoker	1.037	0.599	1.795	0.896				
Clinical stage								
III/IV vs. I/II	2.472	1.662	3.676	<0.001*	2.221	1.478	3.337	<0.001*
Residual tumors								
Yes vs. No	5.025	2.489	10.142	<0.001*	3.522	1.708	7.261	0.001*
TTC9 expression								
High vs. low	1.510	1.038	2.198	0.031*	1.407	0.961	2.061	0.079

Smoking history: 1: lifelong non-smoker; 2: current smoker; 3: current reformed smoker (for >15 years); 4: current reformed smoker (for ≤15 years); 5: current reformed smoker (duration not specified); HR: Hazard ratio. *: $p < 0.005$.

Table 5. Univariate and multivariate analysis of PFI in TCGA-LUAD patients.

Parameters	Univariate analysis				Multivariate analysis			
	HR	95% CI (lower/upper)		P	HR	95% CI (lower/upper)		P
Age (continuous)	0.998	0.984	1.012	0.733				
Gender								
Female vs. Male	0.929	0.706	1.223	0.601				
Smoking history								
Smoker vs. non-smoker	0.970	0.654	1.440	0.881				
Clinical stage								
III/IV vs. I/II	1.622	1.180	2.230	0.003*	1.420	1.019	1.978	0.038*
Residual tumors								
Yes vs. No	3.312	1.780	6.162	<0.001*	2.717	1.423	5.186	0.002*
TTC9 expression								
High vs. low	1.724	1.304	2.278	<0.001*	1.726	1.300	2.290	<0.001*

Smoking history: 1: lifelong non-smoker; 2: current smoker; 3: current reformed smoker (for >15 years); 4: current reformed smoker (for ≤15 years); 5: current reformed smoker (duration not specified); HR: Hazard ratio. *: $p < 0.005$.

3.4. The TTC9 mRNA expression was regulated by DNA amplification and hypomethylation in LUAD

After determining the prognostic value of TTC9 in LUAD, we next explored its biological function and mechanism. In-depth RNA-seq data from the CCLE and TCGA-LUAD was conducted to explore the possible mechanism of dysregulated TTC9 expression in LUAD. First, we examined the relationship between TTC9 mRNA expression and DNA copy number data in 53 LUAD cell lines. As shown in Figure 2A, TTC9 mRNA expression was positively, although not significantly (p = 0.0657),
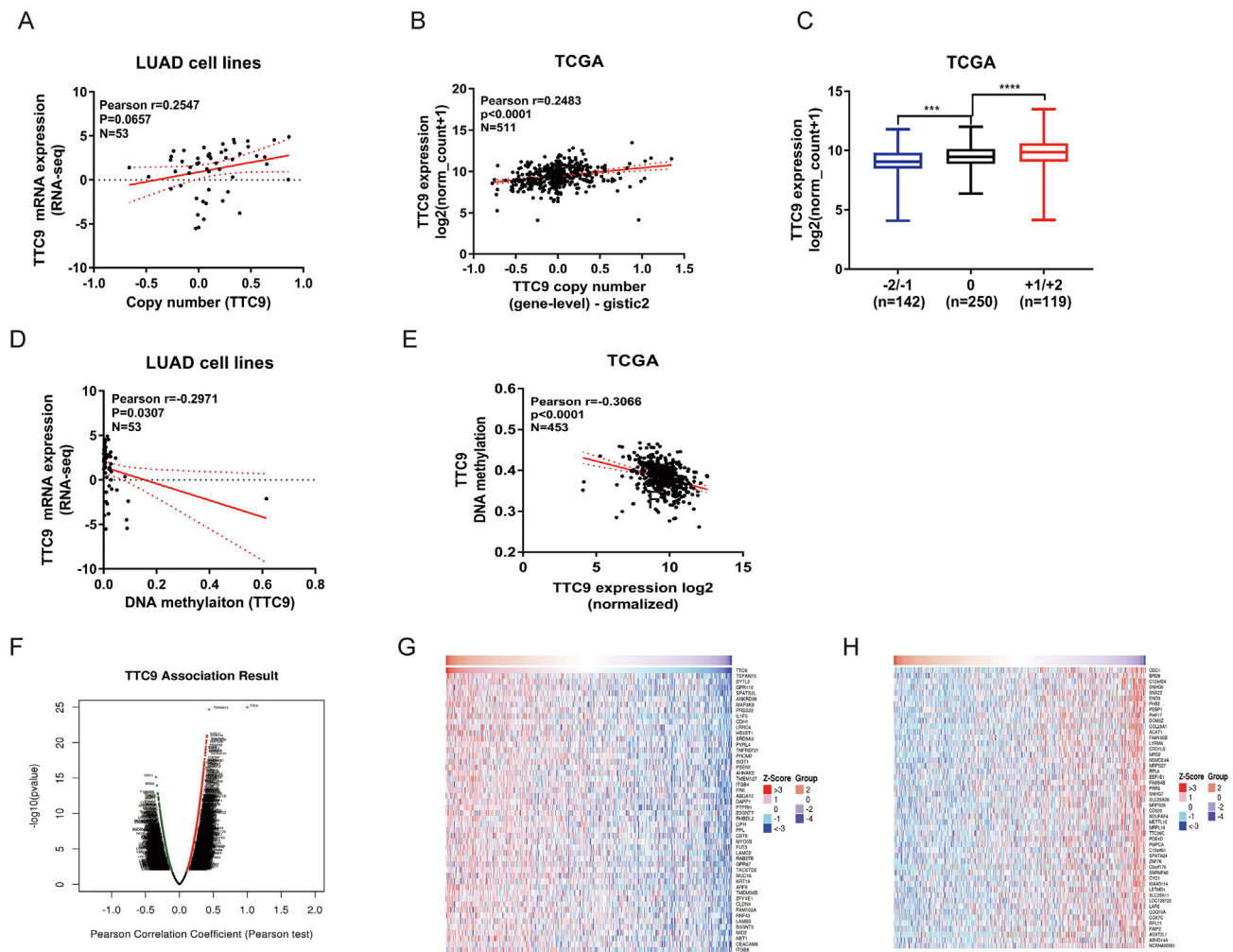
Figure 2. The possible mechanism of TTC9 gene regulation in LUAD. (A) Correlation between TTC9 mRNA expression and DNA copy number in LUAD cell lines (n = 53, p = 0.0657). (B) The expression of TTC9 mRNA was positively associated with DNA copy number (n = 511, p < 0.0001). (C) DNA amplification was correlated with TTC9 mRNA expression. (D) The expression of TTC9 mRNA was negatively associated with DNA methylation level in 53 LUAD cell lines (p = 0.0307 (E) the expression of TTC9 mRNA was negatively associated with DNA methylation (n = 453, p < 0.0001). (F) Volcano plot showing DEGs significantly correlated with TTC9 (FDR <0.01, P < 0.05). (G–H) Heatmaps showing the top 50 genes in LUAD with positive (G) and negative (H) correlations. Pearson correlation test and Welch's t test were performed. *p < 0.05, **p < 0.01, ***p < 0.001.

correlated with copy number. Next, we investigated the relationship between TTC9 mRNA expression and DNA copy number variants (CNV) in 511 primary tumor samples and 21 normal lung samples from the TCGA-LUAD database. The results found that a significant and positive correlation existed between the two parameters (p < 0.0001) (Figure 2B). Among these cases with CNV, 119 (23.3%) cases had DNA amplification and 142 (27.8%) cases had DNA deletion, which were respectively associated with the upregulation and downregulation of TTC9 mRNA expression (Figure 2C). In addition, the relationship between TTC9 mRNA expression and DNA methylation in 53 LUAD cell lines from the CCLE is shown in Figure 2D. TTC9 mRNA expression was negatively correlated with DNA methylation (p = 0.0307). Furthermore, a similar result was obtained when using regression analysis based on the TCGA-LUAD dataset (p < 0.0001, Figure 2E).

3.5. Enrichment analysis of gene sets co-expressed with TTC9 in lung adenocarcinoma

To investigate the possible biological function and molecular mechanism of TTC9 involved in LUAD, we used LinkedOmics to analyze RNA-seq data from 515 LUAD patients in the TCGA. The LinkFinder module of LinkedOmics was performed to identify DEGs that co-expressed with

TTC9 gene in LUAD. A volcano plot showed DEGs negatively (green dots) and positively (red dots) associated with TTC9 in patients with LUAD (FDR <0.01, Figure 2F). The top 50 significant genes with positive or negative correlations with TTC9 were shown in the heatmap (Figure 2G-H). The top 3 genes positively correlated with TTC9 were TSPAN15, SYTL2 and GPR110 (Supplementary 1A). Similarly, there were significantly up-regulated in tumor tissues compared with normal tissues in LUAD (Supplementary 1B).

The LinkInterpreter module of LinkedOmics was used for GSEA analysis to explore the meaningful GO terms and signal pathway enrichment results (top 10) in LUAD. As shown in Figure 3A, by GSEA of genes positively co-expressed with TTC9, the KEGG pathway analysis revealed that some critical cancer-related signaling pathways were significantly enriched, such as 'P53 signaling pathway', 'mTOR signaling pathway', 'ECM receptor interaction' and so on. In addition, these genes were mainly involved in the biological processed of 'homotypic cell-cell adhesion', 'epidermis/skin development', 'ephrin receptor signaling pathway' and so on (Figure 3B). The genes were mainly located in the 'protein complex involved in cell adhesion', 'basal part of cell', 'baso-lateral plasma membrane', and 'actin cytoskeleton' (Figure 3C). For molecular function, enrichment results showed that these genes were mainly involved in 'extracellular matrix binding', 'cell adhesion mediator
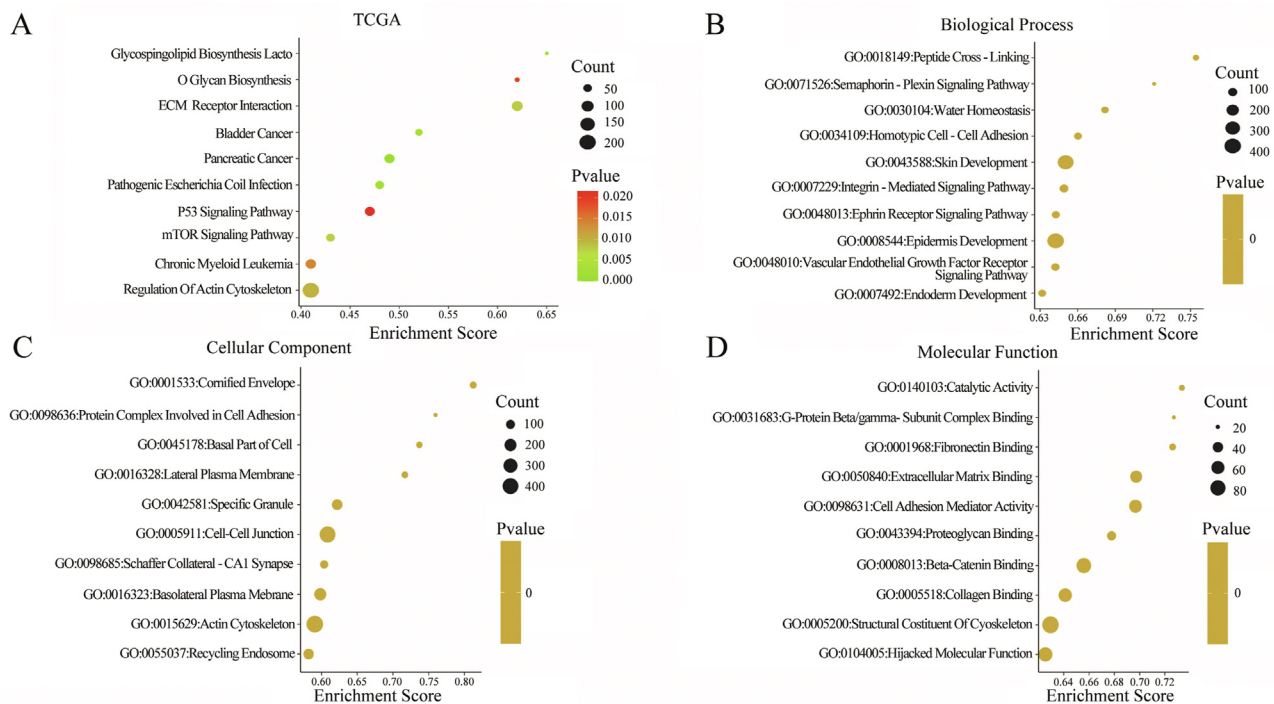
Figure 3. Enrichment analysis of DEGs co-expressed with TTC9 in LUAD. (A) Bubble plot showing the top 10 KEGG pathway enrichment results by GSEA. (B–D) Bubble plots showing the top 10 enrichment results in terms of biological processes, cellular component and molecular function for TTC9 co-expressed genes by GSEA in LUAD.

activity', 'β-catenin/collagen binding', and 'structural components of the cytoskeleton' (Figure 3D).

3.6. Relationship between TTC9 mRNA expression and tumor microenvironment

The prognosis of LUAD is highly correlated with various indicators of the human immune system. To further explore the potential correlation between TTC9 and immune regulation, several algorithms (including CIBERSORT, xCELL, TIMER, EPIC, QUANTISEQ, MCP-COUNTER) based on the gene expression profiles was used for predicting the type and proportion of tumor-infiltrating immune cells (TIICs) in LUAD. As shown in Figure 4, TTC9 expression was negatively correlated with tumor purity activated NK cells, CD8+ T cells, follicular helper T cells, and γδ T cells, and plasma B cells (all p < 0.05). Whereas, TTC9 mRNA expression was positively correlated with neutrophils, M0 phase macrophages, M1 macrophages, M2 phase macrophages, regulatory T cells, bone marrow-derived suppressor cells, cancer-associated fibroblasts, monocytes, CD4+ T cells, myeloid dendritic cells, and mast cells (all p < 0.05).

Furthermore, the effect of TIICs on the survival of LUAD patients was assessed using the "Survival" module in the TIMER database. The results are shown in Figure 5A, the patients with a high proportion of B cells had significantly better OS than those with a low proportion of B cells in LUAD (p < 0.001). Dendritic cell infiltration was negatively associated with OS of LUAD patients (P = 0.048). There were no significant differences observed between CD8+ T cell, CD4+ T cell, macrophage, neutrophil and OS in LUAD. Further analysis showed that LUAD patients with high TTC9 expression and high infiltration levels of CD4+ Th2 cells or bone marrow-derived suppressor cells had significantly poorer OS. Whereas, patients with high TTC9 expression and low myeloid dendritic cell infiltration had a poorer OS (all p < 0.05, Figure 5B–D).

Finally, by datamining in TISIDB database, the expression of TTC9 mRNA expression in different immune subtypes was investigated. There were significant differences in the expression of C1 (wound healing), C2

(interferon-γ dominant), C3 (inflammation), C4 (lymphocyte depletion), C6 (TGF-β dominant) (Figure 5E).

3.7. Effect of TTC9 on proliferation, migration and invasion of LUAD cells

The expression levels of TTC9 mRNA was examined in four LUAD cell lines (namely A549, NCI-H1975, PC9, and H1299) and human normal lung epithelial cell (namely BEAS-2B). The results demonstrated that TTC9 was expressed at the highest expression levels in PC9 cells (Figure 6A). So, PC9 cells were selected for subsequent lentiviral transfection and functional experiment. The efficiency of TTC9 inhibition in stably transfected PC9 cells was examined by qPCR and Western blot assays (Figure 6B–D). CCK-8 assay was used to investigate the effect of TTC9 down-regulation on the viability of PC9 cells. As shown in Figure 6E, knockdown of TTC9 expression in PC9 cells caused a significant decrease in cell viability compared with that in sh-NC cells.

Furthermore, we explored the effect of TTC9 on cell migration and invasion of LUAD cells. The results of cell migration assay and the wound healing assay indicated that the migratory ability of sh-TTC9 PC9 cells was significantly decreased compared with that of control cells (Figure 6F–I). We also assessed the effect of TTC9 down-regulation on invasion ability of LUAD cells. As shown in Figure 6J and K, the invasive capacity of sh-TTC9 PC9 cells was significantly reduced when compared with that of sh-NC PC9 cells in the Matrigel invasion assay. These results suggested that knockdown of TTC9 expression inhibited cell proliferation, migration, and invasion of LUAD cells *in vitro*.

3.8. Effect of TTC9 on the cell cycle and cell apoptosis of LUAD cells

We performed flow cytometry to evaluate the effect of TTC9 on cell cycle and apoptosis of LUAD cells. In the sh-NC group, the proportion of cells in G1 phase, S phase, and G2/M phase were 90.46 ± 0.32%, 3.86 ± 0.21%, and 5.68 ± 0.11%, respectively. In contrast, the percentages in sh-TTC9 cells were 79.49 ± 0.6%, 2.93 ± 0.02%, and 17.59 ± 0.61%, respectively (Figure 5L, M). These results indicated that knockdown of
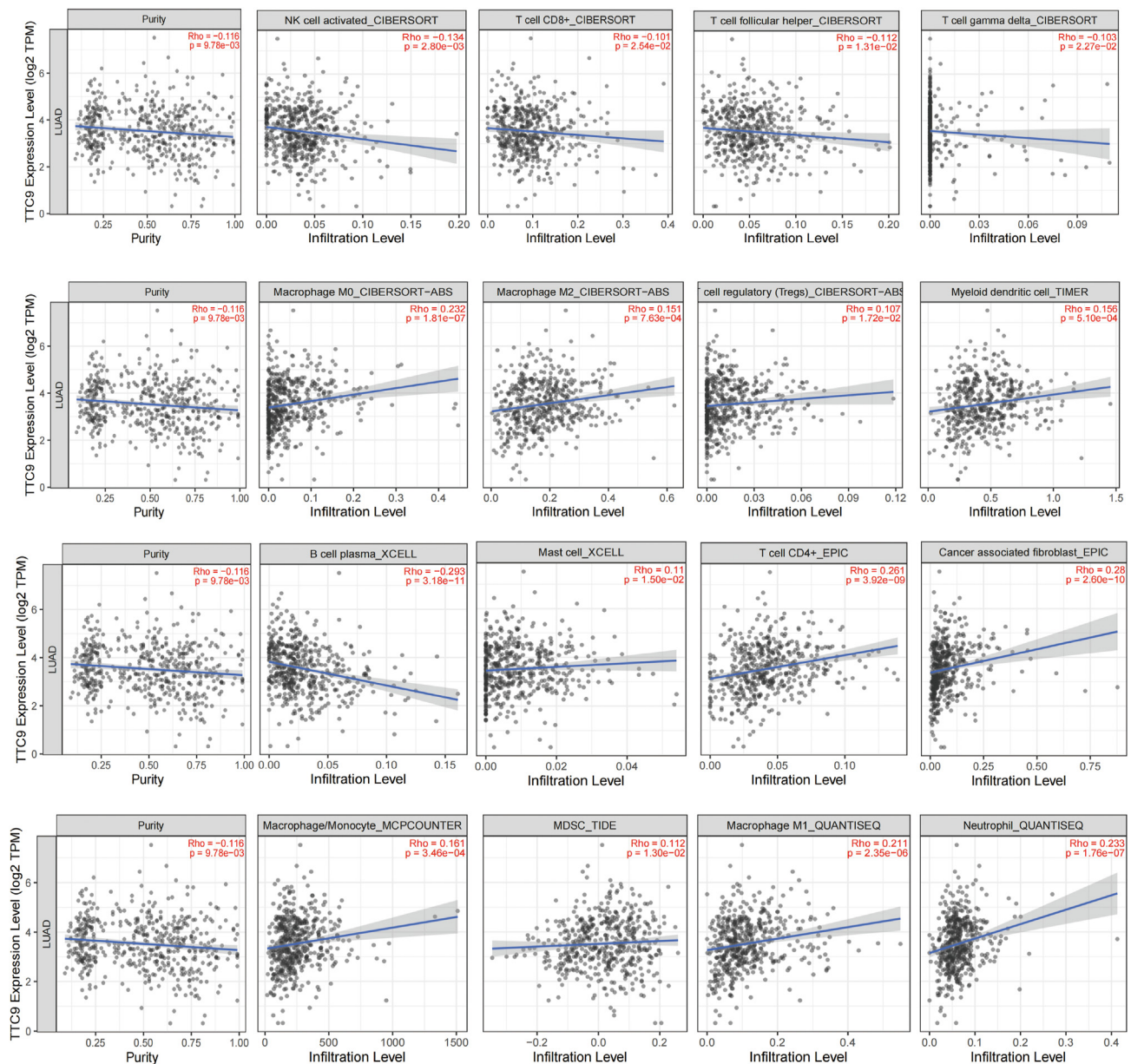
Figure 4. Correlation between TTC9 and tumor-infiltrating immune cells in LUAD. Scatter plots showing correlation between TTC9 expression and the proportion levels of activated NK cells, CD8+ T cells, follicular helper T cells, γδ T cells, M0 macrophages, M2 macrophages, regulatory T cells, myeloid dendrites Correlation of infiltration levels of cytoplasmic cells, plasma cells, mast cells, CD4+ T cells, tumor-associated fibroblasts, monocytes-macrophages, myeloid-derived suppressor cells, and neutrophils in LUAD based on the TIMER database. Spearman's rank correlation test was performed.

TTC9 reduced the proportion of PC9 cells in the G1 and S phases and increased that of cells in the G2/M phase, leading to cell cycle arrest. In addition, the decrease of TTC9 levels led to an increase in the rate of PC9 cell apoptosis when compared with that of cells in the negative control group ($p < 0.05$; Figure 6N, O).

3.9. TTC9 regulates cell apoptosis, and EMT through the p38 MAPK signaling pathway

P38 MAPKs, as a family of 'stress-activated' serine/threonine kinases, are involved in human cells in response to events related to injury repair, extracellular stress stimuli, dynamic remodeling of the actin skeleton, and cell cycle [26, 27, 28]. Previous studies have shown that TTC9 is regulated by p38 inhibitors in breast cancer cells [5]. Accordingly, in the present study, we investigated whether downregulation of TTC9 expression affects the p38 MAPK pathway in LUAD. As shown in

Figure 7A–F, compared with that in sh-NC PC9 cells, the expression of p38 and p-p38 was significantly reduced in sh-TTC9 PC9 cells. In contrast, the expression of caspase-3 and BAX was higher in sh-TTC9 PC9 cells than in sh-NC cells, indicating that inhibition of TTC9 induced the apoptosis of PC9 cells. In addition, compared with the negative control cells, the expression of N-cadherin was downregulated, while the expression of E-cadherin was upregulated in sh-TTC9 group. Taken together, these results suggested that TTC9 might play a role in the development, progression, migration and invasion of LUAD through the p38 MAPK pathway, thereby modulating both EMT and cell apoptosis-related processes.

3.10. Effect of TTC9 on the tumorigenicity of LUAD cells in vivo

The above-mentioned *in vitro* experimental results indicated thatTTC9 knockdown could inhibit the proliferation of LUAD cells. A
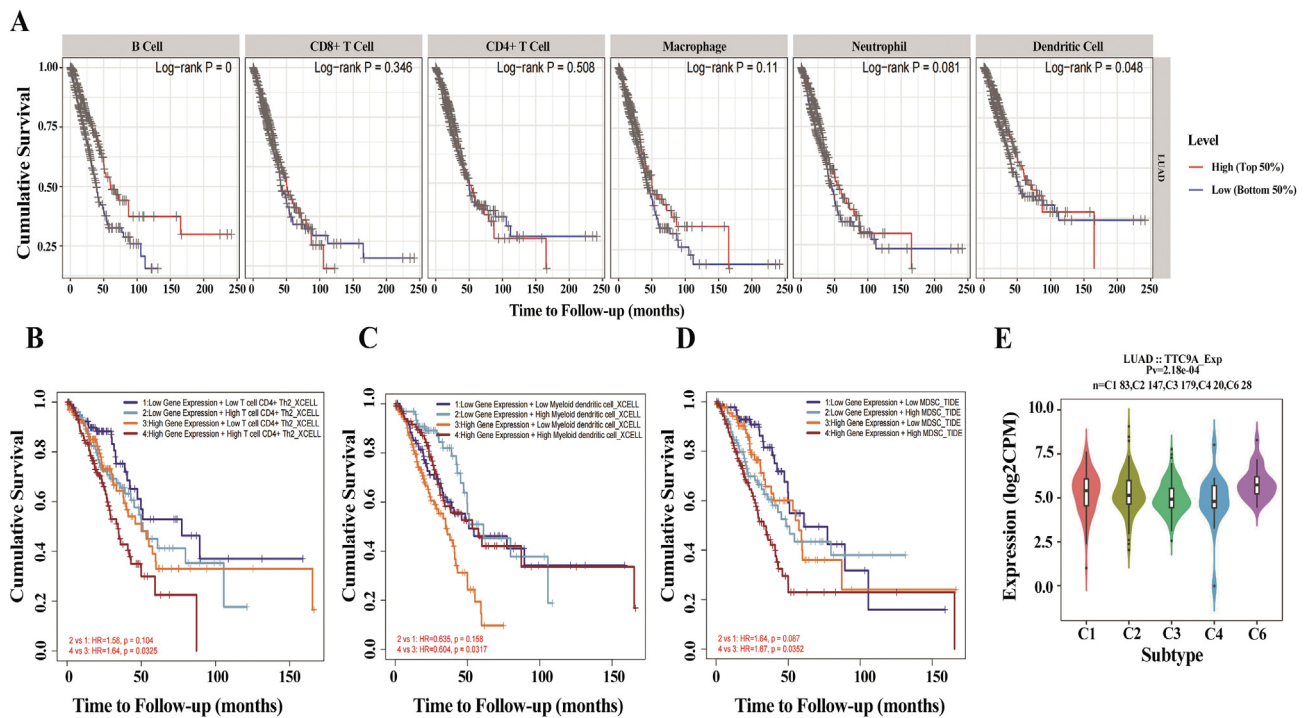
Figure 5. Relationship between TTC9 expression, immune infiltration and survival in patients with LUAD. (A) Kaplan-meier curves of LUAD patients with different types of immune cell infiltration levels using TIMER. (B) Kaplan-meier curve of LUAD patients with TTC9 expression and CD4+ T cell infiltration level analyzed using xCELL. (C) Kaplan-meier curve of LUAD patients with TTC9 expression and myeloid dendritic cell infiltration level analyzed using xCELL. (D) Kaplan-meier curve of LUAD patients with TTC9 expression and infiltration levels of myeloid-derived suppressor cells analyzed using TIDE. (E) Expression of TTC9 mRNA in different immune subtypes. C1: wound healing; C2: interferon-γ dominant; C3: inflammation; C4: lymphocyte depletion; C5: immune silencing; C6: TGF-β dominant. Log-rank test and Welch's t test were performed.

LUAD xenograft model in nude mice was established to verify if these findings were reproducible *in vivo*. The results revealed that tumorigenicity, tumor weight, and tumor volume were all reduced ($p < 0.05$) in mice injected with sh-TTC9 LUAD cells compared with that in control mice. Consistent with the *in vitro* results, these findings indicated that knockdown of TTC9 inhibited the proliferative capacity of LUAD cells *in vivo* (Figure 7G–I).

4. Discussion

Cancer is a disease in which features of normal cell behavior and morphology are lost or disturbed. Uncontrolled cell proliferation, migration, and invasion are typical manifestations of cancer. The actin cytoskeleton is a key player supporting cell motility, and many proteins that interact directly or indirectly with actin have been shown to significantly influence tumor cell migration and metastasis [29]. Yamada et al [30] found that immunologic analysis of 70 primary oral squamous-cell carcinoma and 10 normal oral mucosa specimens collected demonstrated upregulation of F-actin-binding protein Cortactin expression in primary oral squamous-cell carcinoma. Trovik et al [31] found that overexpression of the cellular microtubule filamentous regulatory Stathmin protein was associated with lymph node metastasis and poor survival in endometrial cancer. These results suggested that actin could control the progression of cancer by regulating the proliferation and migration of cancer cells.

The tropomyosin Tm5NM1 is a major cytoskeletal component and is thought to be involved in regulating mesenchymal cell motility. Tm5NM1 stabilizes actin Fascin and contributes to fibrous adhesion by regulating actin filaments [32]. Recent studies have shown that changes in the structure of the actin cytoskeleton are associated with oncogenic mechanisms [33]. TTC9 protein is a binding protein of tropomyosin Tm5NM-1 in physiological function. Interestingly, TTC9 can bind to Tm5NM-1 to regulate the contractility and focal adhesion of actin

filaments, thereby affecting the process of cell development and participating in the migration and focal adhesion of breast cancer cells [6]. However, up to now, the expression and role of TTC9 in LUAD are poorly understood. Does TTC9 protein, a Tropomyosin chaperone that stabilizes actin, could affect migration and invasion of LUAD cells? Further research is required.

In the present study, we explored for the first time the expression profile, biological function and underlying mechanism of TTC9 in LUAD. In the pan-cancer expression profiles, the mRNA expression of TTC9 was found to be significantly up-regulated in a variety of malignant tumors, including LUAD. The protein expression level of TTC9 in lung adenocarcinoma was higher than that in normal lung tissue detected by immunohistochemistry. These results confirmed the overexpression of TTC9 in lung adenocarcinoma. TCGA-LUAD data were further integrated to analyze the clinical significance of TTC9 mRNA expression in patients with LUAD. The results revealed that high TTC9 mRNA expression was significantly correlated with female, lymph node invasion, residual tumor and outcome status. But, there was no significant difference between TTC9 expression and distant metastasis, which might be related to the failure to collect tissue samples in most patients with distant metastases. Therefore, TTC9 may be involved in the carcinogenesis and progression of LUAD. Moreover, according to the clinical prognostic analysis of TCGA database, high TTC9 mRNA expression was significantly associated not only with poor OS, but also with poor DFI, DSS, and PFI. The results of univariate and multivariate Cox regression analysis confirmed that high TTC9 mRNA expression was an independent risk factor for unfavorable prognosis in patients with LUAD. To sum up, TTC9 could act as a promising diagnostic and prognostic biomarker for LUAD.

Abundant evidence indicates that functional abnormalities of genetic material and epigenetic regulation is closely related to carcinogenesis [34, 35, 36]. Gene mutations in cancer cells alter the structure and stability of the genome, together with genetic lesions, lead to carcinogenesis [37]. Up to now, the molecular mechanisms underlying TTC9 dysregulation in
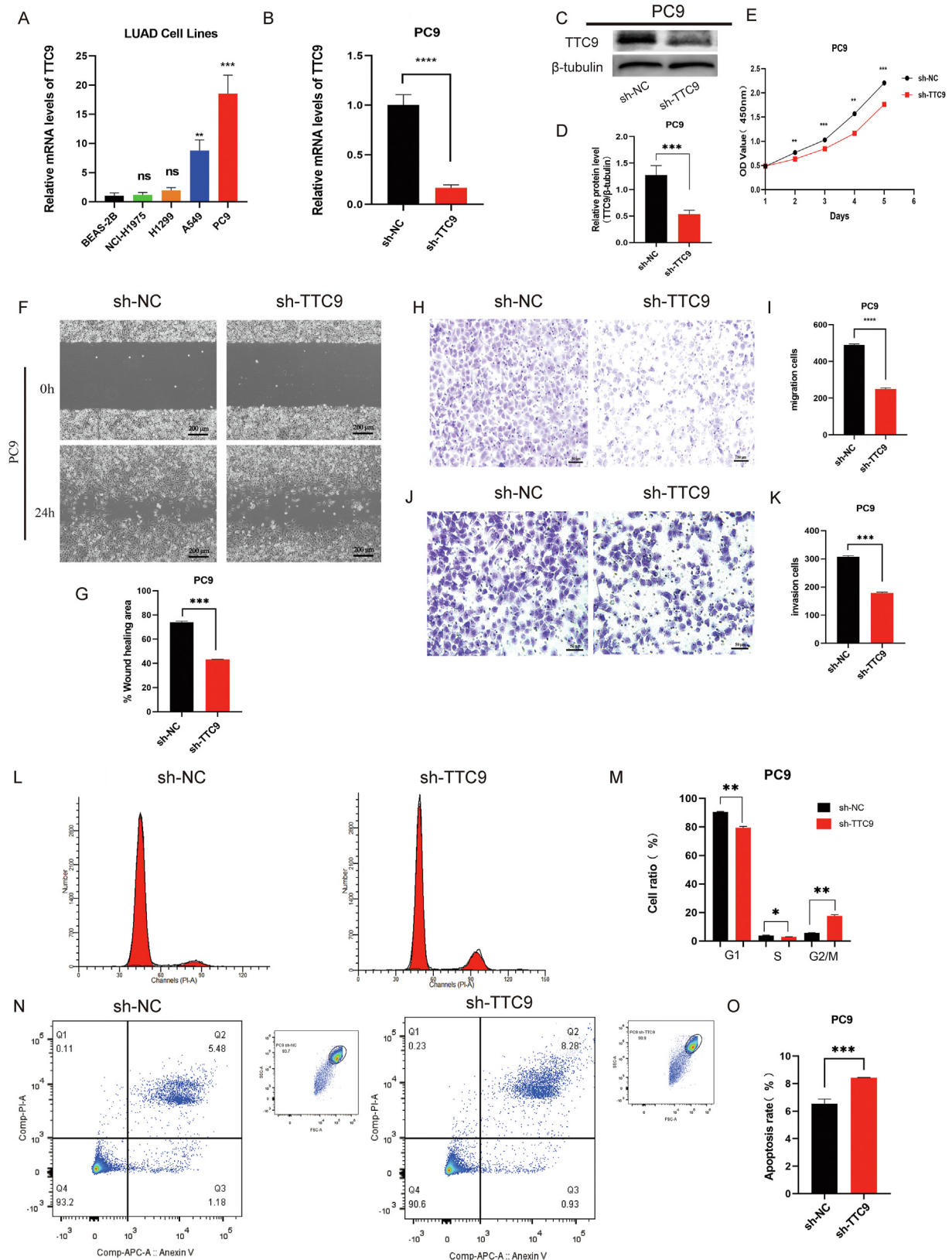
Figure 6. The role of TTC9 in LUAD cells. (A) qPCR assay for detecting the endogenous expression of TTC9 mRNA in BEAS-2B, H1299, A549, NCI-H1975, and PC9 cells. (B) qPCR-based detection of TTC9 mRNA levels in sh-TTC9 and sh-NC PC9 cells. (C–D) TTC9 protein levels in sh-TTC9 and sh-NC PC9 cells were detected by Western blot assay. (E) The effects of TTC9 knockdown on the proliferation of PC9 cells. (F–G) Wound healing assay results showing the effect of TTC9 knockdown on the migratory capability of PC9 cells (×100 magnification, Scale bars: 200 μm). (H–I) Transwell assay results showing the effect of TTC9 knockdown on the migratory capability of PC9 cells (×200 magnification, Scale bars: 50 μm). (J–K) A Matrigel invasion assay was used to examine the effect of TTC9 knockdown on the invasive capacity of PC9 cells (×200 magnification, Scale bars: 50 μm). (L–M) Cell cycle distribution was detected in PC9 cells. (N-O) Cell apoptosis was detected in PC9 cells by flow cytometry using Annexin V/PI double staining. Welch's t test and Wilcoxon rank sum test were used. *$p < 0.05$, **$p < 0.01$, ***$p < 0.001$, ****$p < 0.0001$.
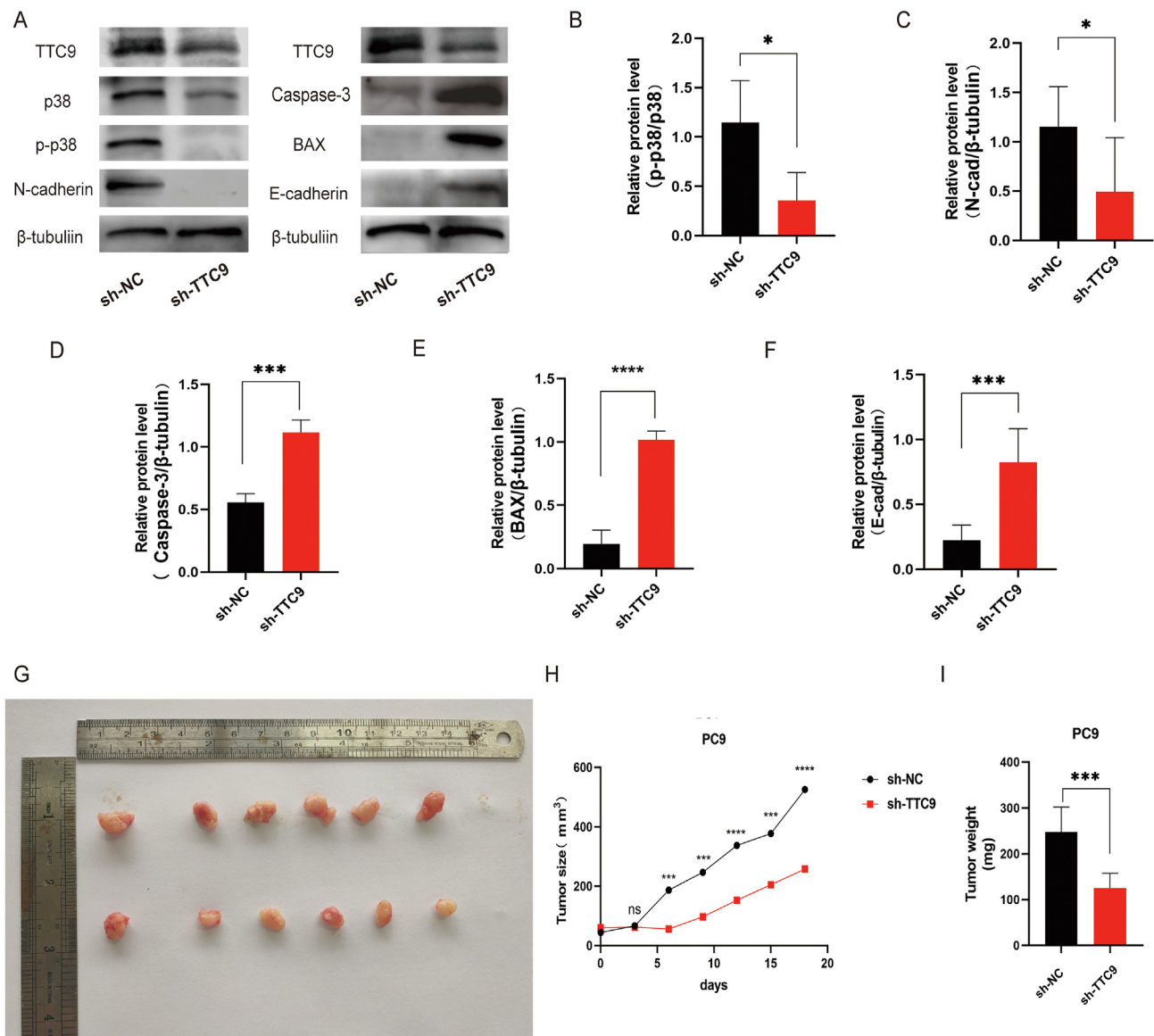
Figure 7. Effect of TTC9 on signaling pathway-related proteins and tumorigenicity of LUAD cells. (A) Western blots showing the protein expression of the p38 MAPK, apoptosis signaling pathway-related factors and EMT-associated markers in PC9 cells transfected with sh-TTC9. (B–F) Histograms showing relative expression levels of aforementioned proteins in LUAD. (G) Knockdown of TTC9 inhibited tumor growth in PC9 xenografted nude mice. Comparison of the sizes (H) and weights (I) of xenografted tumors derived from sh-TTC9 and sh-NC PC9 groups. Welch's t test and Wilcoxon rank sum test were used. *p < 0.05, **p < 0.01, ***p < 0.001, ****p < 0.0001.

tumors have not been fully understood. By collecting relevant data from bioinformatics database, we analyzed the biological behavior of LUAD that might be affected by TTC9 expression from the aspects of epigenetics, molecular pathway and immune gene. Firstly, we investigated the relationship between TTC9 mRNA expression and DNA methylation levels by datamining TCGA and CCLE database. TTC9 mRNA expression was negatively associated with DNA methylation at both tissue and cellular levels, indicating that the abnormal expression and dysregulation of TTC9 gene in LUAD might be related to the hypomethylation of the patients' genome. Secondly, the possible molecular mechanism of TTC9 in LUAD was further analyzed using GSEA. By using LinkedOmics platform, we identified the DEGs co-expressed with TTC9 in LUAD. The most significant genes that positively correlated to TTC9 were TSPAN15, SYTL2 and GPR110. They were significantly up-regulated in primary LUAD tumor tissues, and were reported to play critical role in the regulation of cell development, growth, invasion, metastasis, and exocytosis [38, 39, 40]. Furthermore. enrichment analysis focused on ECM receptor interaction,

extracellular matrix binding and regulation of cell adhesion mediator activity, and mainly involved in cell adhesion and then regulate actin cytoskeleton-related activities.

Furthermore, we investigated the correlation between TTC9 expression and TIICs in patients with LUAD using various algorithms. TTC9 expression was significantly associated with many types of lymphocyte in LUAD. Interestingly, the expression of TTC9 gene was positively correlated with the level of macrophage and dendritic cells infiltration in the TIMER database, and the LUAD patients with high TTC9 expression and myeloid dendritic cell infiltration showed better OS. In the immune response, dendritic cell is the most powerful antigen-presenting cell, with the unique ability to transport tumor antigens to the lymph nodes to initiate T cell activation. However, due to the dysregulation of immunosuppressive molecules and cytokines, as well as the existence of multiple immunosuppressive mechanisms such as immunomodulatory subsets, it is difficult for B and T cells to fully exert their killing function in the tumor microenvironment [41]. The association of a large number

of immune cell biomarkers with TTC9 was analyzed using various immune cell databases, suggesting that TTC9 might be involved in the complex coordination among immune cells. TTC9 might play a role in regulating humoral and cellular immune responses, which in turn affected the tumor microenvironment of LUAD.

We were encouraged by the aforementioned results based on bioinformatics analysis that TTC9 was likely to be a promising biomarker in LUAD. To explore the biological function of TTC9 gene, we used lentivirus interference technology to silence the expression of TTC9 gene in LUAD cell line. The results of CCK-8 and mice xenograft model experiments showed that silencing TTC9 gene significantly inhibited the proliferation of LUAD cells *in vitro* and *in vivo*. Knockdown of TTC9 promoted cell apoptosis, inhibited cell migration and invasion, and induced cell cycle arrest in G2 phase. Uncontrolled cell cycle, apoptosis, ad cell metastasis are important manifestations of tumor development. Mitogen-activated protein kinase (MAPKs) family is involved in the proliferation and migration of lung cancer [42, 43, 44]. The p38 MAPK signaling pathway is an important pathway that can be activated by different stimuli or environmental stresses. It plays key role in tumor development, including regulating the proliferation, differentiation, apoptosis and survival, of tumor cells. Epithelial-mesenchymal transition (EMT) is a conserved and reversible biological process characterized by the loss of cell polarity, adhesion, and cell compactness, this changes the morphology of epithelial cells to mesenchymal-like spindle cells and results in their migratory capacity and invasiveness [45]. The plasticity of EMT is hijacked by cancer cells and will contribute to the development of malignant tumors. In the apoptotic process, Bax is a pro-apoptotic protein of the BCL protein family, both of which regulate apoptosis in cells by controlling mitochondrial permeability [46]. Caspase-3 is a member of the cysteine - aspartic acid protease (caspase) family. Sequential activation of caspases plays a central role in the execution-phase of cell apoptosis [47]. The hyperphosphorylation activation of the p38 MAPK signaling pathway drives the initiation and progression of biological processes, including EMT and apoptosis, in many human cancers [48]. In previous studies, Cao et al [5] mentioned that TTC9 is regulated by p38 kinase inhibitors in breast cancer. It is therefore speculated that TTC9 might regulate the initiation and progression of LUAD through the p38-related signaling pathways. In the present study, Western blot results confirmed that inhibition of TTC9 resulted in the dephosphorylation of p38 MAPK signaling pathway and decreased the expression of p-p38 and p38. Knockdown of TTC9 increased the expression of BAX, Caspase-3 and E-cadherin, while decreased the expression of N-cadherin. These findings revealed that inhibition of TTC9 could promote cell apoptosis, inhibit the proliferation, invasion and metastasis of LUAD cells through p38 MAPK signaling pathway. Therefore, our findings highlighted the candidate eligibility of TTC9 as an effective target for therapeutic intervention in LUAD.

Although some innovative results have been achieved, there are still limitation in this study. For example, there is a lack of sufficient tissue samples to investigate the relationship between TTC9 protein expression and clinicopathologic features. In bioinformatics analysis, some correlation coefficients appear to be low and more experimental validation is needed in future studies. As the topic of this study is the expression profiles and biological function of TTC9 in patients with LUAD. The in-depth relevance and molecular mechanism of TTC9 involvement in tumor-infiltrating immune cells should be examined in future experiments. The role and mechanism of TTC9 in the p38 MAPK signaling pathway needs to be verified by more comprehensive and more experiments in the future.

Declarations

Author contribution statement

Xiaoyue Huang; Lingyu Jiang: Performed the experiments; Analyzed and interpreted the data; Contributed reagents, materials, analysis tools or data; Wrote the paper.

Zhaoke Wen: Analyzed and interpreted the data; Contributed reagents, materials, analysis tools or data.

Mingqing Yuan: Conceived and designed the experiments; Analyzed and interpreted the data; Wrote the paper.

Yonglong Zhong: Conceived and designed the experiments; Analyzed and interpreted the data; Contributed reagents, materials, analysis tools or data; Wrote the paper.

Data availability statement

Data associated with this study has been deposited at TCGA database (https://portal.gdc.cancer.gov/) and GEO database (https://www.ncbi.nlm.nih.gov/geo/).

Declaration of interests statement

The authors declare no conflict of interest.

Additional information

Supplementary content related to this article has been published online at https://doi.org/10.1016/j.heliyon.2022.e11194.

References

[1] H. Sung, J. Ferlay, R.L. Siegel, et al., Global cancer statistics 2020: GLOBOCAN estimates of incidence and mortality worldwide for 36 cancers in 185 countries, CA A Cancer J. Clin. 71(2021), 209-249.

[2] M.C. Turner, Z.J. Andersen, A. Baccarelli, et al., Outdoor air pollution and cancer: an overview of the current evidence and public health recommendations, CA A Cancer J. Clin. (2020).

[3] C. Allemani, T. Matsuda, V. Di Carlo, for CONCORD Working Group, Global surveillance of trends in cancer survival 2000-14 (CONCORD-3): analysis of individual records for 37 513 025 patients diagnosed with one of 18 cancers from 322 population-based registries in 71 countries, Lancet 391 (2018) 1023–1075.

[4] G.P. Gupta, J. Massagué, Cancer metastasis: building a framework, Cell 127 (2006) 679–695.

[5] S. Cao, J.K. Iyer, V. Lin, Identification of tetratricopeptide repeat domain 9, a hormonally regulated protein, Biochem. Biophys. Res. Commun. 345 (2006) 310–317.

[6] S. Cao, G.H. Ho, V.C. Lin, Tetratricopeptide repeat domain 9A is an interacting protein for tropomyosin Tm5NM-1, BMC Cancer 8 (2008) 231.

[7] S. Shrestha, Y. Sun, T. Lufkin, et al., Tetratricopeptide repeat domain 9A negatively regulates estrogen receptor alpha activity, Int. J. Biol. Sci. 11 (2015) 434–447.

[8] C.T.T. Bach, G. Schevzov, N.S. Bryce, et al., Tropomyosin isoform modulation of focal adhesion structure and cell migration, Cell Adhes. Migrat. 4 (2) (2010) 226–234.

[9] J.M. Percival, J.A. Hughes, D.L. Brown, et al., Targeting of a tropomyosin isoform to short microfilaments associated with the Golgi complex, Mol. Biol. Cell 15 (1) (2004) 268–280.

[10] S. Shrestha, S. Cao, V.C. Lin, The local microenvironment instigates the regulation of mammary tetratricopeptide repeat domain 9A during lactation and involution through local regulation of the activity of estrogen receptor α, Biochem. Biophys. Res. Commun. 426 (2012) 65–70.

[11] Cancer Genome Atlas Research Network, J.N. Weinstein, E.A. Collisson, G.B. Mills, K.R. Shaw, B.A. Ozenberger, K. Ellrott, I. Shmulevich, C. Sander, J.M. Stuart, The cancer genome Atlas pan-cancer analysis project, Nat. Genet. 45 (10) (2013) 1113–1120.

[12] D.P. Nusinow, J. Szpyt, M. Ghandi, C.M. Rose, E.R. McDonald, M. 3rd Kalocsay, J. Jané-Valbuena, E. Gelfand, D.K. Schweppe, M. Jedrychowski, J. Golji, D.A. Porter, T. Rejtar, Y.K. Wang, G.V. Kryukov, F. Stegmeier, B.K. Erickson, L.A. Garraway, et al., Quantitative proteomics of the cancer cell line Encyclopedia, Cell 180 (2) (2020), 387–402.e16.

[13] J. Barretina, G. Caponigro, N. Stransky, et al., The Cancer Cell Line Encyclopedia enables predictive modelling of anticancer drug sensitivity, Nature 483 (7391) (2012) 603–607.

[14] D.S. Chandrashekar, B. Bashel, S. Balasubramanya, C.J. Creighton, I. Ponce-Rodriguez, B. Chakravarthi, S. Varambally, UALCAN: a portal for facilitating tumor subgroup gene expression and survival analyses, Neoplasia 19 (8) (2017) 649–658.

[15] S.V. Vasaikar, P. Straub, J. Wang, B. Zhang, LinkedOmics: analyzing multi-omics data within and across 32 cancer types, Nucleic Acids Res. 46 (D1) (2018) D956–D963.

[16] Z. Tang, B. Kang, C. Li, T. Chen, Z. Zhang, GEPIA2: an enhanced web server for large-scale expression profiling and interactive analysis, Nucleic Acids Res. 47 (W1) (2019) W556–W560.

[17] D. Aran, Z. Hu, A.J. Butte, xCell: digitally portraying the tissue cellular heterogeneity landscape, Genome Biol. 18 (1) (2017) 220.

[18] J. Racle, K. de Jonge, P. Baumgaertner, D.E. Speiser, D. Gfeller, Simultaneous enumeration of cancer and immune cell types from bulk tumor gene expression data, Elife 6 (2017), e26476.

[19] A.M. Newman, C.L. Liu, M.R. Green, A.J. Gentles, W. Feng, Y. Xu, C.D. Hoang, M. Diehn, A.A. Alizadeh, Robust enumeration of cell subsets from tissue expression profiles, Nat. Methods 12 (5) (2015) 453–457.

[20] C. Plattner, F. Finotello, D. Rieder, Deconvoluting tumor-infiltrating immune cells from RNA-seq data using quanTIseq, Methods Enzymol. 636 (2020) 261–285.

[21] E. Becht, N.A. Giraldo, L. Lacroix, B. Buttard, N. Elarouci, F. Petitprez, J. Selves, P. Laurent-Puig, et al., Erratum to: estimating the population abundance of tissue-infiltrating immune and stromal cell populations using gene expression, Genome Biol. 17 (1) (2016) 249.

[22] A.R. Abbas, K. Wolslegel, D. Seshasayee, Z. Modrusan, H.F. Clark, Deconvolution of blood microarray data identifies cellular activation patterns in systemic lupus erythematosus, PLoS One 4 (7) (2009), e6098.

[23] P. Jiang, S. Gu, D. Pan, J. Fu, A. Sahu, X. Hu, Z. Li, N. Traugh, X. Bu, B. Li, J. Liu, G.J. Freeman, M.A. Brown, K.W. Wucherpfennig, X.S. Liu, Signatures of T cell dysfunction and exclusion predict cancer immunotherapy response, Nat. Med. 24 (10) (2018) 1550–1558.

[24] B. Li, E. Severson, J.C. Pignon, H. Zhao, T. Li, J. Novak, P. Jiang, H. Shen, J.C. Aster, S. Rodig, S. Signoretti, J.S. Liu, X.S. Liu, Comprehensive analyses of tumor immunity: implications for cancer immunotherapy, Genome Biol. 17 (1) (2016) 174.

[25] A. Subramanian, P. Tamayo, V.K. Mootha, S. Mukherjee, B.L. Ebert, M.A. Gillette, et al., Gene set enrichment analysis: a knowledge-based approach for interpreting genome-wide expression profiles, Proc. Natl. Acad. Sci. U. S. A 102 (43) (2005) 15545–15550.

[26] J. Gao, Y. Zhao, Y. Lv, et al., Mirk/Dyrk1B mediates G0/G1 to S phase cell cycle progression and cell survival involving MAPK/ERK signaling in human cancer cells, Cancer Cell Int. 13 (2013) 2.

[27] H. Ji, H.W. Lu, Y.M. Li, et al., Twist promotes invasion and cisplatin resistance in pancreatic cancer cells through growth differentiation factor 15, Mol. Med. Rep. 12 (3) (2015) 3841–3848.

[28] M. Madrid, E. Gómez-Gil, J. Cansado, Negative control of cytokinesis by stress-activated MAPK signaling, Curr. Genet. 67 (5) (2021) 715–721.

[29] A. Hall, The cytoskeleton and cancer, Cancer Metastasis Rev. 28 (1–2) (2009) 5–14.

[30] S. Yamada, G. Kawasaki, A. Mizuno, et al., Overexpression of cortactin increases invasion potential in oral squamous cell carcinoma, Pathol. Oncol. Res. 16 (4) (2010) 523–531.

[31] J. Trovik, E. Wik, I.M. Stefansson, et al., Stathmin overexpression identifies high-risk patients and lymph node metastasis in endometrial cancer, Clin. Cancer Res. 17 (10) (2011) 3368–3377.

[32] C.T. Bach, G. Schevzov, N.S. Bryce, et al., Tropomyosin isoform modulation of focal adhesion structure and cell migration, Cell Adhes. Migrat. 4 (2) (2010) 226–234.

[33] S. Sharma, C. Santiskulvong, J. Rao, et al., The role of Rho GTPase in cell stiffness and cisplatin resistance in ovarian cancer cells, Integr. Biol.: Quantit. Biosci. Nano Macro 6 (6) (2014) 611–617.

[34] S. Horike, K. Mitsuya, M. Meguro, et al., Targeted disruption of the human LIT1 locus defines a putative imprinting control element playing an essential role in Beckwith-Wiedemann syndrome, Hum. Mol. Genet. 9 (14) (2000) 2075–2083.

[35] T. Eggermann, N. Schönherr, E. Meyer, et al., Epigenetic mutations in 11p15 in Silver-Russell syndrome are restricted to the telomeric imprinting domain, J. Med. Genet. 43 (7) (2006) 615–616.

[36] K. Buiting, Prader-Willi syndrome and Angelman syndrome, Am. J. Med. Genet. Part C, Seminars Med. Genet. 154C (3) (2010) 365–376.

[37] A.P. Feinberg, R. Ohlsson, S. Henikoff, The epigenetic progenitor origin of human cancer, Nat. Rev. Genet. 7 (1) (2006) 21–33.

[38] S. Cai, Y. Deng, H. Peng, et al., Role of tetraspanins in hepatocellular carcinoma, Front. Oncol. 11 (2021), 723341.

[39] T. Izumi, Physiological roles of Rab27 effectors in regulated exocytosis, Endocr. J. 54 (5) (2007) 649–657.

[40] B. Ma, J. Zhu, J. Su, F. Pan, Y. Ji, L. Luan, J. Huang, Y. Hou, The role of GPR110 in lung cancer progression, Ann. Transl. Med. 8 (12) (2020) 745.

[41] S.T. Paijens, A. Vledder, M. de Bruyn, et al., Tumor-infiltrating lymphocytes in the immunotherapy era, Cell. Mol. Immunol. 18 (4) (2021) 842–859.

[42] A. Cuadrado, A.R. Nebreda, Mechanisms and functions of p38 MAPK signalling, Biochem. J. 429 (3) (2010) 403–417.

[43] D. Zhao, T. Zhang, X.M. Hou, et al., Knockdown of fascin-1 expression suppresses cell migration and invasion of non-small cell lung cancer by regulating the MAPK pathway, Biochem. Biophys. Res. Commun. 497 (2) (2018) 694–699.

[44] N. Thompson, J. Lyons, Recent progress in targeting the Raf/MEK/ERK pathway with inhibitors in cancer drug discovery, Curr. Opin. Pharmacol. 5 (4) (2005) 350–356.

[45] T. Kim, A. Veronese, F. Pichiorri, et al., p53 regulates epithelial-mesenchymal transition through microRNAs targeting ZEB1 and ZEB2, J. Exp. Med. 208 (5) (2011) 875–883.

[46] S. Zhang, N. Liu, M. Ma, et al., Methionine enkephalin (MENK) suppresses lung cancer by regulating the Bcl-2/Bax/caspase-3 signaling pathway and enhancing natural killer cell-driven tumor immunity, Int. Immunopharm. 98 (2021), 107837.

[47] T.J. Fan, L.H. Han, R.S. Cong, et al., Caspase family proteases and apoptosis, Acta Biochim. Biophys. Sin. 37 (11) (2005) 719–727.

[48] Y. Sun, W.Z. Liu, T. Liu, et al., Signaling pathway of MAPK/ERK in cell proliferation, differentiation, migration, senescence and apoptosis, J. Recept. Signal Transduct. Res. 35 (6) (2015) 600–604.